



Adsorption mechanism of emerging and conventional phenolic compounds on graphene oxide nanoflakes in water



Hepsiba Niruba Catherine^{a,b}, Ming-Han Ou^b, Basavaraju Manu^a, Yang-hsin Shih^{b,*}

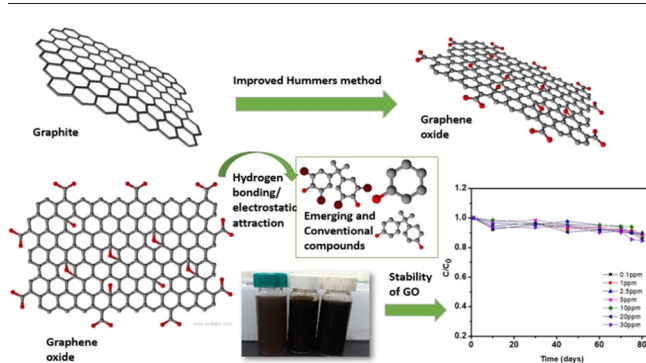
^a Department of Civil Engineering, National Institute of Technology Karnataka, Surathkal 575025, India

^b Department of Agricultural Chemistry, National Taiwan University, Taipei 106, Taiwan

HIGHLIGHTS

- Graphene oxide nanoflakes we synthesized have a high suspension stability in water.
- Graphene oxide (GO) surface was studied by several spectroscopic methods.
- Adsorption mechanisms of emerging compounds (ECs) on GO were illustrated.
- π - π interactions and hydrophobic interactions dominate the adsorption process.
- GO with ECs could lead to their spread in aquatic environment.

GRAPHICAL ABSTRACT



ARTICLE INFO

Article history:

Received 1 February 2018

Received in revised form 30 March 2018

Accepted 31 March 2018

Available online xxxx

Keywords:

Emerging contaminants

Graphene oxide

Phenolic compounds

Adsorption mechanism

Electrostatic attraction

Hydrogen-bonding

ABSTRACT

Emerging contaminants (ECs) such as bisphenol A (BPA), 4-nonylphenol (4-NP) and tetrabromobisphenol A (TBBPA) have gained immense attention worldwide due to their potential threat to humans and environment. Graphene oxide (GO) nanomaterial is considered as an important sorbent due to its exceptional range of environmental application owing to its unique properties. GO was also considered as one of ECs because of its potential hazard. The adsorption of organic contaminants such as phenolic ECs on GO affects the stability of GO nanoflakes in water and the fate of organic contaminants, which would cause further environmental risk. Therefore, the adsorption behaviors of emerging and common phenolic compounds (PCs) including phenol, 4-chlorophenol, 2,4-dichlorophenol, 2,4,6-trichlorophenol, 4-NP, BPA and TBBPA on GO nanoflakes and their stability in water were studied. The adsorption equilibrium for all the compounds was reached <10 h and was fitted with Langmuir and Freundlich isotherms. In addition to hydrophobic effect, adsorption mechanisms included π - π bonding and hydrogen bonding interactions between the adsorbate and GO, especially the electrostatic interactions were observed. Phenol has the highest adsorption affinity due to the formation of hydrogen bond. GO has a good stability in water even after the adsorption of PCs in the presence of a common electrolyte, which could affect its transport with organic contaminants in the environment. These better understandings illustrate the mechanism of emerging and common PC interaction with GO nanoflakes and facilitate the prediction of the contaminant fate in the aquatic environment.

© 2018 Elsevier B.V. All rights reserved.

* Corresponding author.

E-mail address: yhs@ntu.edu.tw (Y. Shih).

1. Introduction

Emerging contaminants (ECs) are a new class of identified compounds of rising concern that have been investigated in the past 20 years, mainly comprising pharmaceuticals, surfactants, flame retardants, hormones, and nanomaterials. They are widely detected in many environmental media and raise public concerns because they are toxic and have no regulatory standards (Petrie et al., 2015; Sophia and Lima, 2018; Zhu et al., 2017). ECs are widely found in water supplies and persistent, which could cause an adverse effect to humans (Rivera-Utrilla et al., 2013). These chemicals present in the environment are of more concern as they do not appear individually but mostly as a complex, which lead to synergistic effect (Petrie et al., 2013). ECs like bisphenol A (BPA), 4-nonylphenol (4-NP), tetrabromobisphenol A (TBBPA) and some relative phenolic compounds (PCs) exist in water due to their discharge from industrial, domestic, and agricultural wastewater.

Graphene oxide (GO) nanosheet is a derivative of graphite that contains oxygen bearing functional groups at the edges of the carbon layer. The presence of oxygen-carrying functional groups and high surface area make GO a promising tool for adsorption. Graphene nanomaterials and their derivative reveal excellent performance in the environmental contaminant removal of dyes, organic, inorganic pollutants and heavy metal due to the large theoretical surface area, fast electron transfer and the presence of functional groups (Jiang et al., 2015; Shen et al., 2015). GO has the potential for the elimination of organic compounds containing benzene ring due to strong interaction with π - π system. Its high affinity of PAHs to graphene material was also dominated by π - π stacking (Chowdhury and Balasubramanian, 2014; Wang et al., 2014b).

GO has gained recent attention among researchers due to its significant electronic, mechanical and chemical properties. The huge application of GO has led to the growing concerns of transport of GO in the natural water bodies during the life cycle process (Doudrick et al., 2015). The large-scale usage and production of nanomaterials such as GO have unavoidably lead to its release into the environment, posing a potential threat to health and also increasing its possible interaction with the contaminants in the environment (Johra et al., 2014; Peng et al., 2016). For the toxicity of GO, many biological activities were hampered in the presence of GO in the activated sludge (Ahmed and Rodrigues, 2013). The antibacterial properties of GO to pure bacterial cultures were observed (Mejias Carpio et al., 2012). Furthermore, GO can suspend well in water and hence form colloidal suspension due to the electrostatic repulsion originating by the presence of carboxylic and hydroxyl groups on the GO sheets. It is necessary to examine the colloidal stability and its environmental transport to evaluate its fate and health risk (Li et al., 2008; Yao et al., 2015). Once GO releases into the environment, their adsorption of organic contaminants further influences the fate of both pollutants. The sorption could lead to the enhanced mobility of adsorbed ECs on GO nanomaterials causing an environmental risk. The properties of ECs such as the dissociation constant (pK_a), aromatic ring substitution and solubility will affect its interaction with GO surface. Therefore, the adsorption of organic compounds by GO nanoflakes is required to understand the fate of these organic pollutants in water (Liu et al., 2016; Wu et al., 2014; Zhang et al., 2013).

In the present study, the synthesized GO was used to examine the adsorption behavior of ECs in water and their adsorption mechanism. Conventional phenolic contaminants such as phenol, 4-CP, 2,4, DCP, 2,4,6 TCP were chosen to compare their adsorption behaviors. The chemical compositions and surface morphologies of self-synthesized GO nanoflakes were analyzed. Sorption experiments of on GO nanoflakes were performed to study their sorption behavior and interaction mechanism. A better understanding of the sorption of ECs and PCs with GO will lead to the fate prediction of these contaminants in the environment.

2. Materials and methods

2.1. Chemicals and reagents

Graphite flakes (<20 mm) and potassium permanganate ($KMnO_4$) were purchased from Sigma-Aldrich. Hydrochloric acid (HCl, 37%), sulfuric acid (H_2SO_4 , 98%) and phosphoric acid (H_3PO_4 , 85%) with Grade AR were purchased from Merck. Phenol, 4-chlorophenol (4-CP), 2,4-dichlorophenol (2,4-DCP), 2,4,6-trichlorophenol (2,4,6-TCP), bisphenol A (BPA), 4-nonylphenol (4-NP), and tetrabromobisphenol A (TBBPA) were obtained from Acros. Hydrogen peroxide (30–32%) Grade AR was purchased from Acros chemical company. All solutions were prepared using deionized (DI) water (Millipore, Temecula, CA, USA).

2.2. Preparation of graphene oxide

GO was synthesized by following improved Hummers method (Dreyer et al., 2010; Sahu et al., 2017). In brief, 2.0 g of graphite flakes were added to a mixture 225 mL of sulfuric acid and 25 mL phosphoric acid maintained at a temperature of 35 °C. 5.0 g of potassium permanganate was gradually added to the solution that was maintained at 35 °C and stirred continuously for 10 h. The resultant mixture was cooled in an ice bath, diluted with 225 mL of DI water, then 3 mL of 30% hydrogen peroxide was added to the mixture to remove the residual permanganate. A large number of bubbles will be released and the solution color will be changed to brilliant yellow. The suspension was centrifuged several times and washed with 0.1 N hydrochloric acid and phosphate buffer to remove extra manganese ion. The final solution was washed with DI water to lower the pH value to around 5–7 and then dried in rotary vapor at 45 °C. The GO suspension was prepared by sonication GO sheets in DI water for 2 h.

2.3. Characterization of graphene oxide

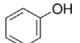
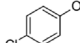
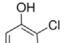
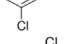
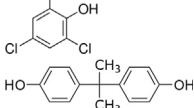
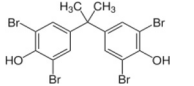
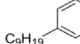
The properties of the GO sample were characterized by using Fourier-transform infrared spectroscopy (FTIR), Raman spectroscopy, and X-ray diffraction (XRD). All experiments were performed at different beamlines in National Synchrotron Radiation Research Center (Taiwan). The surface elemental composition was also accomplished by using X-ray photoelectron spectroscopy (XPS). The morphological characterization was performed by using scanning electron microscopy (SEM, JOEL JSM-7600F) and transmission electron microscopy (TEM, JEOL JEM-200CX). SEM/TEM images of the GO were captured digitally for further size analysis.

The electrophoretic mobility of GO samples at different pH values was measured by Zetasizer Nano ZS dynamic light scattering (DLS, Malvern, MA) and their zeta potentials were calculated according to the Helmholtz-Smoluchowski equation. The sedimentation of GO nanoflakes was determined according to time-resolved optical absorbance by using an ultraviolet-visible spectrophotometer (UV-Vis, CT-2200, Chrom Tech, Inc., Apple Valley, MN, USA) at 230 nm.

2.4. Adsorption experiments

Sorption batch experiments of phenol, 4-CP, 2,4-DCP, 2,4,6-TCP, 4-NP, BPA and TBBPA were all performed in a shaker at 150 rpm at 25 °C in the dark. 4 mL amber vials with PTFE screw cap were added one sorbate and the background solution containing 0.01 M $CaCl_2$ in DI water and 200 mg/L NaN_3 as bio-inhibitor. The physiochemical properties of the pollutants considered in our study are listed in Table 1. The kinetic studies were performed by using 20 mg/L sorbate and 5 mg GO nanoflakes to determine the equilibrium time for each sorbate. The time-dependent adsorption experiments were determined by varying the time from 5 to 1440 min. For isotherms, the vials were prepared as the above by adding various concentrations of sorbate and shaking for >48 h. All experiments were repeated at least three times. The vials

Table 1
Molecular structure and chemical properties of phenolic compounds.

Compound	Structure	Kow	pK _a	Solubility (g/L)
Phenol		1.16	10	86.6
4-Chlorophenol		2.39	9.41	27
2,4-Dichlorophenol		3.17	7.89	4.5
2,4,6-Trichlorophenol		3.7	6.23	0.9
BPA		3.36	9.6	0.03
TBBPA		5.90	7.5	0.00416
4-Nonylphenol		5.76	10.37	0.005

were centrifuged at a speed of 6000 rpm for 10 min and then the supernatants were analyzed by Agilent 1200 HPLC equipped with an UV/VIS detector for phenol (275 nm), 4-CP (286 nm), 2,4-DCP (285 nm), 2,4,6-TCP (284 nm), and TBBPA (280 nm), as well as with a fluorescence detector for BPA and 4-NP (excitation at 220 nm and emission at 315 nm). The adsorption amount, Q_e (mg/g), was determined by the difference of two measurements, the initial concentration, C_0 (mg/L) and the equilibrium concentration, C_e (mg/L), in Eq. (1):

$$Q_e = (C_0 - C_e) V/M \quad (1)$$

where V (mL) is the volume of the solution in the vial, and M (mg) is the mass of GO.

3. Results and discussion

3.1. Characterization of graphene oxide

The SEM and TEM images displayed the wrinkles distributed on the edge of GO nanoflakes (Fig. 1a and b) and also showed a large and flat structure thus creating a potential adsorption site. These wrinkled sheets could result from the presence of oxygen-containing groups on GO (Wang et al., 2014a). Furthermore, from the XRD pattern for GO nanoflakes (Fig. 2a), the diffraction peak of GO at 9.72° confirmed the synthesized GO. The intense peak in Fig. 2a, at 26.82° corresponds to

graphite. The interlayer of graphite expands as oxygen carrying functional groups are incorporated, indicating that the crystalline structure of graphite was destroyed and was completely oxidized to GO. From the XRD data, the difference of these XRD peaks from 10.02 to 26.72 is due to the presence of oxygen-carrying groups (Dimiev and Tour, 2014; Gao et al., 2012).

The functional groups of GO nanoflakes shown in the FTIR spectra (Fig. 2b) have a broad peak at 3320 cm^{-1} due to the O—H stretching, the other main peaks at 1760, 1620, 1420 and 1048 cm^{-1} due to vibration of C=O, aromatic stretching of C=C, benzene ring C=C stretching and alkoxy C—O stretching vibration, respectively. The peak at 1760 cm^{-1} ascribes the stretching vibrations due to C=O in the carbonyl group of GO after oxidation from graphite (Yu et al., 2014). For graphite, the peaks at 1574, 1739 and 1240 cm^{-1} correspond to the benzene ring C=C stretching vibrations, carboxyl C=O, and epoxy C—O vibrations respectively. The presence of enlarged peaks of the oxygenated functional group on GO explains the successful oxidation of GO from graphite (Thirumal et al., 2016).

In Raman spectra (Fig. 2c), graphite had a strong G band at 1579 cm^{-1} and a weak D band at 1360 cm^{-1} (Johra et al., 2014). Compared to graphite, D and G bands of GO had some peak shifts to 1349 and 1582 cm^{-1} , respectively. The G band in GO is shifted to a wavenumber higher than graphite, due to the oxygenation of graphite, that resulted in the formation of sp^3 carbon atoms. Furthermore, the ratio of D band and G band is used to define the degree of disorder and the reduction of graphene (Perumbilavil et al., 2015). The ratio of I_D/I_G of graphite is 0.85 and for GO is 0.99, whose difference raised due to the defects created by the aromatic structure and degree of disorders. The increase in the ratio of I_D/I_G of graphite to GO confirms the presence of oxygen contain groups to the graphitic (Wu et al., 2016).

Zeta potential is an important factor to characterize the colloidal dispersion stability and also infer the magnitude and sign of the double layer surrounding the colloidal particle. Values of zeta potential more than +30 mV or −30 mV are considered to lead to stable colloids due to electrostatic repulsion (Konkena and Vasudevan, 2012). Zeta potentials of GO samples at different pH values decreased with the increasing solution pH (Fig. 3). The aqueous dispersion of GO nanoflakes was found to be stable in the neutral pH, which resulted from a high negative value of zeta potential (−50.3 mV). It also confirmed the presence of negatively charged functional groups we observed on the edges of GO surface since carbonyl, epoxy and hydroxyl groups lead to extreme hydrophilicity with negative charge density (Krishnamoorthy et al., 2013; Liu et al., 2016).

To investigate the stability of prepared GO nanoflakes, UV-visible spectroscopy was also used. The sedimentation curves are recorded for various concentrations of BPA are determined by measuring its optical absorbance (Fig. 4). GO dispersion exhibits a good stability. In the

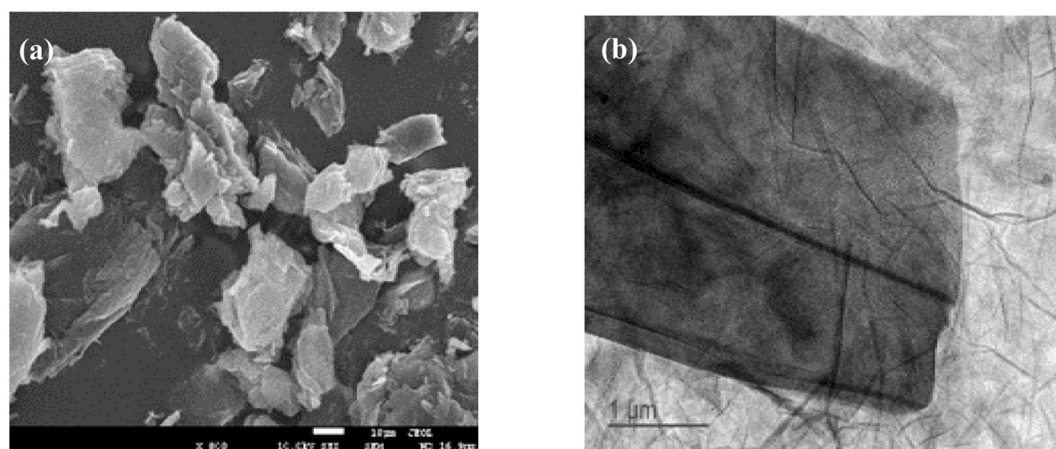


Fig. 1. (a) SEM and (b) TEM of GO.

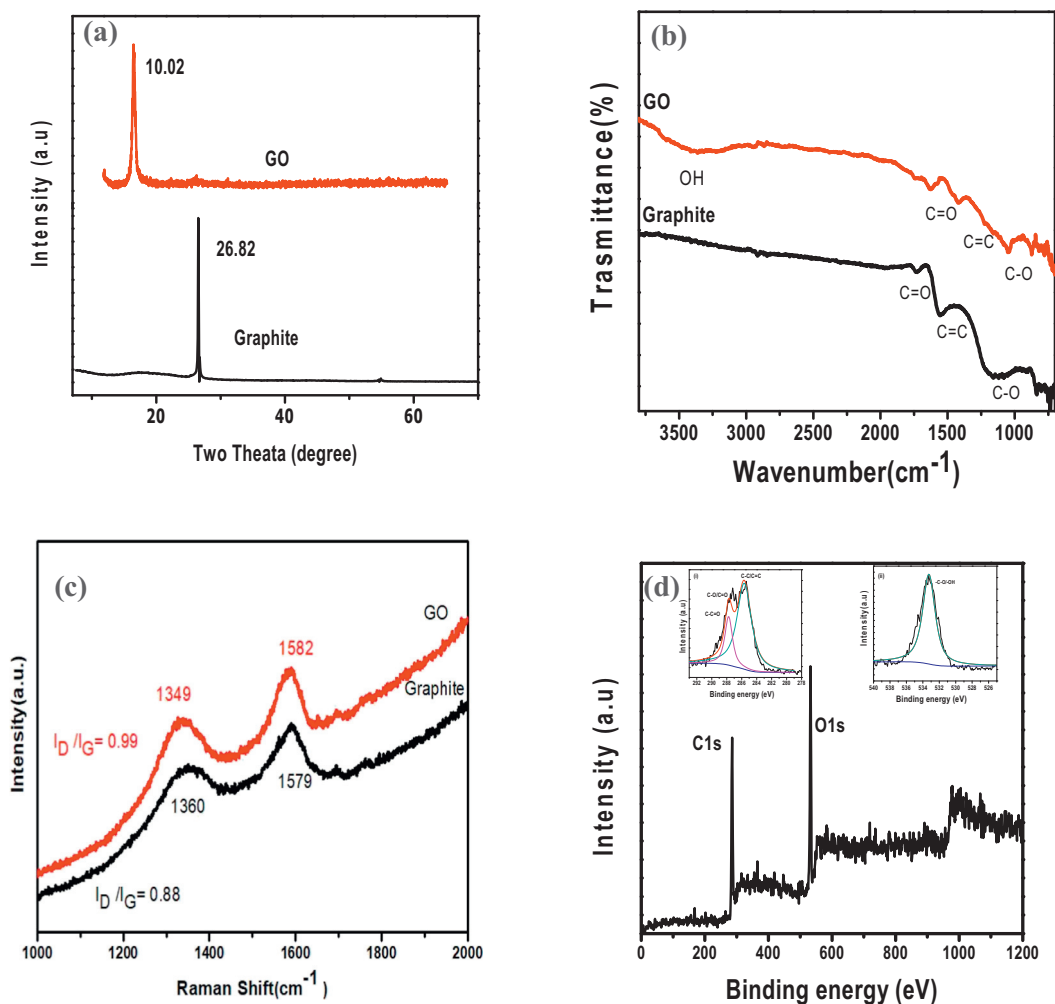


Fig. 2. (a) XRD, (b) FTIR, (c) Raman spectra of graphite and GO and (d) XPS spectrum of GO (i) carbon (C1s) peaks of GO and (ii) oxygen (O1s) peaks of GO.

inserted photograph of Fig. 4, the GO dispersion appears dark, indicating significant part of GO remains stable. In the presence of the other chemicals in water, GO shows a similar stability (data not shown). The similar stability of GO without these phenolic chemicals was shown in

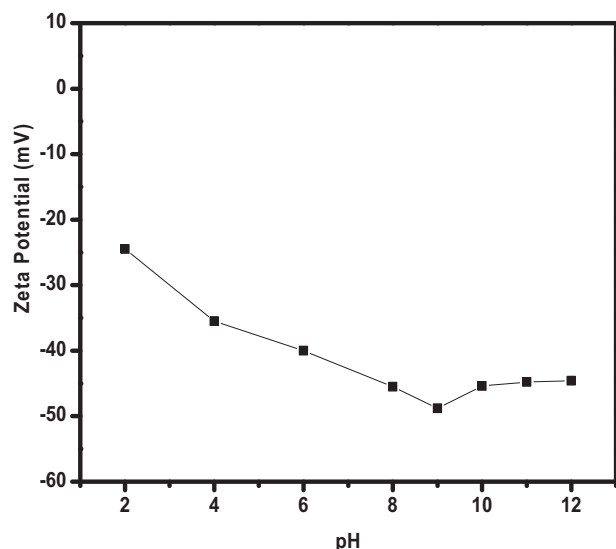


Fig. 3. Zeta potentials of GO under different pH conditions.

Liang et al. (2016). Several nanoparticles (NPs) are not stable in water (Tso et al., 2010). Furthermore, Hsiung et al. (2016) indicated TiO₂ NPs settle down with 1 h and Peng et al. (2017) even found the stabilized ZnO NPs lost >20% by absorbance measurement with 10 days. Compared to these nanomaterials, our GO seems very stable in water. GO has special lamellar structure and good dispersion stability that improve the aqueous stability. This stability of GO can have a substantial effect on its toxicity, fate, and environmental transport once it adsorbed organic contaminants.

The surface properties or defects of GO were also analyzed, the distribution of C1s of GO (Fig. 2d) shows the highest intensity binding energy at 287.8 belonging to the carbonyl functional group, whereas the other peak at 286.7 corresponding to C—C/C—C in aromatic rings. The distribution of O1s XPS spectra of GO (Fig. 2d(ii)) was also analyzed and showed the peak at 533.2 corresponding to —C—O and —OH groups. Examining the nitrogen adsorption/desorption isotherms of GO and its pore distribution, our GO was a mesoporous material according to IUPAC classification (Fig. S1) (Veerakumar et al., 2017; Wu et al., 2014). The BET surface area of GO was 0.727 m²/g.

3.2. Adsorption kinetics of phenolic contaminants on graphene oxide

The adsorption kinetics of the seven phenolic compounds on GO was shown in Fig. 5. For these seven chemicals, the rapid sorption occurred during the first 30 min of the reaction time, thereafter followed a slow rate for 120–400 min, and attained the saturation in 480 min for all compounds. The rate of adsorption increases with the increase in

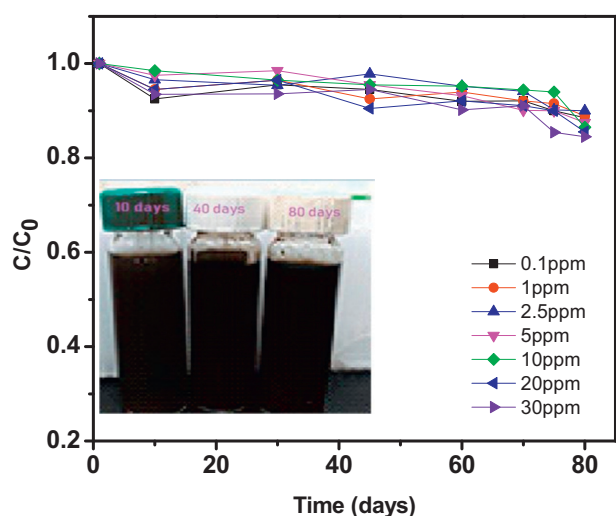


Fig. 4. Sedimentation curve of GO with different concentrations of BPA in the presence of 0.01 M CaCl_2 . (The inside picture is the images of GO at 10 ppm in water after 90 days.)

time, similar kinetics pattern was also observed by (Xu et al., 2012), indicating that graphene-based materials possess a fast adsorption. The adsorption kinetics of PCs on GO nanoflakes is divided into three stages, the first stage of film diffusion (fast diffusion), the second stage of intraparticle diffusion (slow sorption), and the final stage of dynamic equilibrium (Phatthanakittiphong and Seo, 2016). Our kinetic results were fitted to both pseudo-first-order model and the pseudo-second-order one. The pseudo-first order kinetic model (Eq. (2)) and pseudo-second-order kinetic model (Eq. (3)) are shown:

$$\ln(q_e - q_t) = \ln q_e - k_1 t \quad (2)$$

$$t/q_t = 1/k_2 q_e^2 + t/q_e \quad (3)$$

where q_e (mg/g) is the adsorption concentration at equilibrium, q_t (mg/g) is the adsorption concentration at time t , k_1 is the pseudo-first-order model constant of adsorption rate ($1/\text{min}$), k_2 ($\text{g}/(\text{mg min})$) in Eq. (3) is the pseudo-second-order model constant of adsorption rate.

The pseudo-first-order rate constants for these seven compounds on GO are in the range of 0.012 – 0.087 min^{-1} (Table S1). 2,4,6-TCP had the highest pseudo-first-order rate constant. The pseudo-second-order rate constant for BPA on our GO was slightly smaller than that on Belle's GO (Bele et al., 2016), which could result from the less surface area of our GO than theirs. The pseudo-first and pseudo-second order kinetics both describe the adsorption kinetic curves well. From the regression

coefficients (R^2) shown in Table S1, the pseudo-second order kinetics seems slightly better than pseudo-first one.

3.3. Adsorption isotherms of phenolic compounds onto graphene oxide

For TBBPA and 4-NP, the adsorption seemed to increase with the increasing aqueous concentration in the range we studied (Fig. 6). A similar pattern was observed for BPA, 2,4,6-TCP, DCP, CP, and phenol. Although the adsorption of all PCs by GO seemed not to follow a linear pattern, their adsorption on GO increased with the increase of the concentration of PCs (Fig. 6). The two isotherm models, Langmuir and Freundlich isotherms, are used to describing the adsorption of these PCs and ECs onto GO surfaces.

$$Q_e = \frac{b q_m C_e}{1 + b C_e} \quad (4)$$

$$Q_e = K_f C_e^{1/n} \quad (5)$$

where Q_e (mg/g) is the adsorbed amount of PCs onto GO, C_e (mg/L) is the equilibrium concentrations of PCs in the solution, b (L/mg) is related to the energy of adsorption, q_m (mg/g) is the Langmuir monolayer adsorption capacity, K_f is Freundlich adsorption constant and n is exponential Freundlich coefficient.

Fig. S2 presented these fitting data by two isotherms for phenolic compounds, indicating Freundlich model seems better than Langmuir one. However, their relative parameters were listed in Table S2, Langmuir model fitted the sorption isotherms slightly better than the Freundlich model, suggesting the possible single layer adsorption on GO. The adsorption isotherms were normalized according to the surface area of the adsorbent (Fig. 7). The synchronized occurrence of monolayer adsorption could happen in the presence of a flat structure of GO surface was confirmed by its SEM image (Fig. 1b). Only a few studies have compared the adsorption interactions between GO and organic contaminants with different physiochemical properties and functional groups, GO having a flat surface act an ideal platform for the π - π interaction and hydrophobic effect (Wu et al., 2016).

GO exhibited a similar type of adsorption affinities to six compounds including 4-CP, 2,4-DCP, 2,4,6-TCP, BPA, TBBPA and 4-NP. Among these compounds, phenol had the highest adsorption capacity on GO. Due to the formation of hydrogen bonds between the phenolic molecules and the oxygen-carrying functional groups on GO surface (Kalita et al., 2011), polar PCs could have similar adsorption ability as more nonpolar PCs such as chlorinated ones. Furthermore, our q_m values of some hydrophobic chemicals such as TBBPA and 4-NP were less than others. The q_m values of chlorophenols decreased with the increase of their chlorination, suggesting the hydrophilic surface of GO we prepared. A

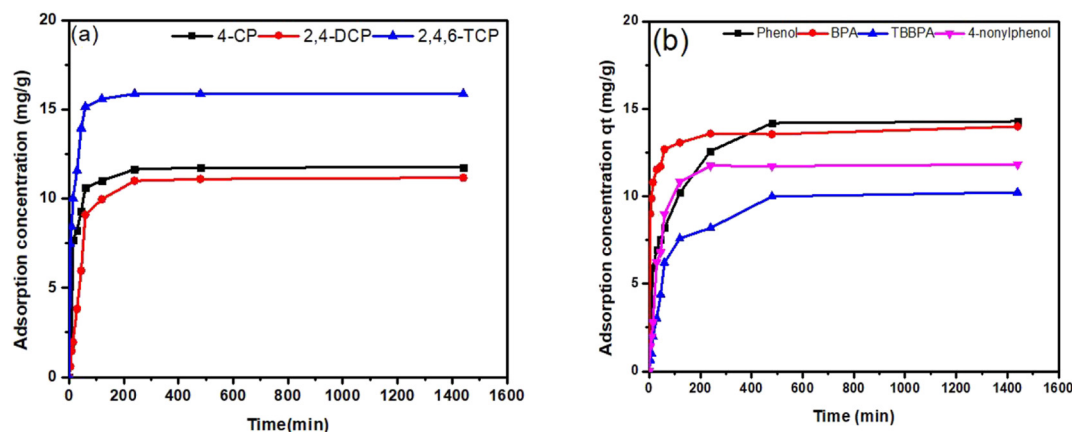


Fig. 5. (a) Adsorption kinetics of 4-chlorophenol, 2,4-dichlorophenol, 2,4,6-trichlorophenol (b) phenol, BPA, 4-nonylphenol and TBBPA on GO.

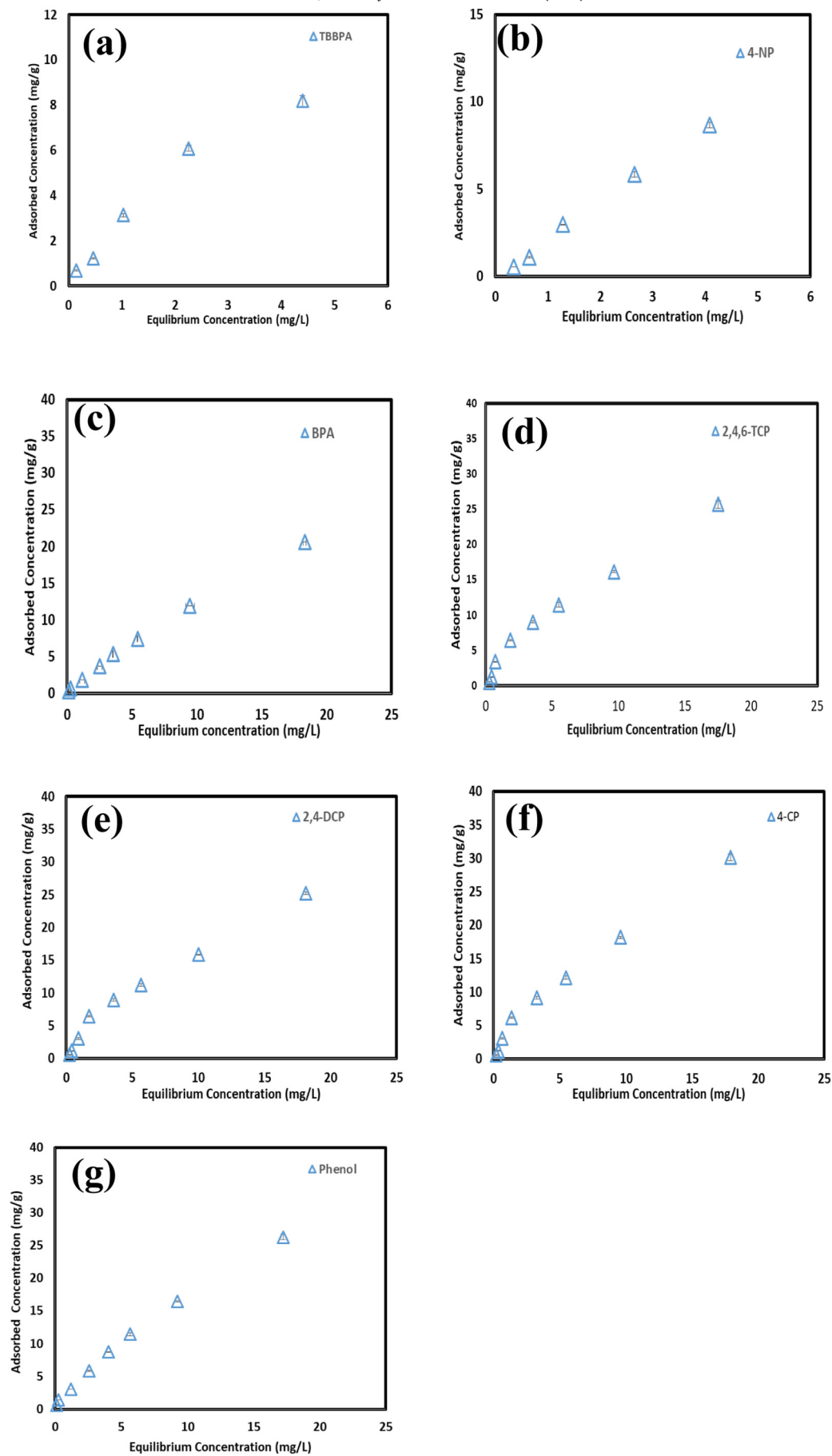


Fig. 6. Adsorption isotherms of (a) TBBPA, (b) 4-NP, (c) BPA, (d) 2,4,6-TCP, (e) 2,4-DCP, (f) 4-CP, and (g) phenol on GO.

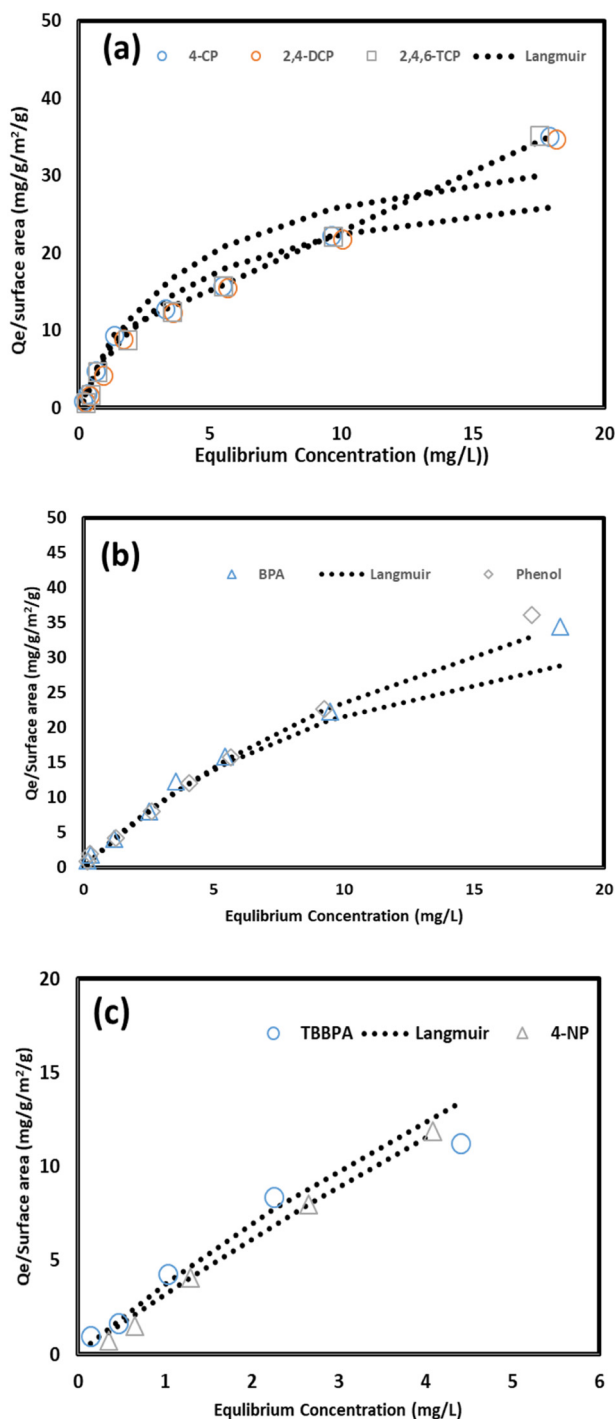


Fig. 7. Surface area-normalized sorption isotherms of (a) 4-CP, 2,4-DCP and 2,4,6-TCP, (b) BPA and phenol (c) TBBPA and 4-NP on GO.

similar result such as a higher adsorption of TCP than trichlorobenzene was observed.

3.4. Adsorption mechanism of phenolic compounds onto graphene oxide

The adsorption mechanisms of organic contaminants on graphene-based materials at the molecular level are dependent on the adsorbate-adsorbate, adsorbate-solvent which largely depend on physical, chemical and electrostatic interaction (Moreno-Castilla, 2004). The π - π interaction, hydrophobic effect, hydrogen bonding, electrostatic interaction and dispersion (Van der Waals) are commonly used to

demonstrate the adsorption mechanism of organic chemicals on graphene-based materials. In addition, π - π electron donor-acceptor (EDA) can also be a primary adsorption enhancement mechanism for phenolic compounds with strong π -electron donating ability or strong π -withdrawing ability, due to the interaction of adsorbate molecule with π region of graphene surface. In the present study, the adsorption affinity for BPA seemed slightly higher than DCP and TCP (q_m values in Table S2) could be due to the π - π EDA interaction of one more benzene ring of BPA than CPs with graphene oxide.

The oxygen carrying functional groups of GO will lead to the formation of a hydrogen bond with the water molecule, thus making GO more hydrophilic and suppressing the adsorption of GO with the pollutants (Sun et al., 2013). The main mechanism governing the interaction could also be due to the π - π interaction as each carbon atom of GO has a π -electron perpendicular to the GO surface (Zhang et al., 2013). Furthermore, the availability of adsorptive sites on GO for the adsorption of PCs is provided by the surface properties and defects such as oxygen moieties (Apul et al., 2013). The interaction of hydrogen-bond donor and acceptor (HDA) also contributed the adsorption. Since GO nanoflakes had oxygen carrying functional groups, PCs, OH-containing compounds, have a strong HDA ability thus exhibiting HAD interaction with GO surface. The greater interactions between phenol with GO could result from its lowest hydrophobicity, π - π and HDA interactions. Pei et al. (2013) also indicated the HDA interaction between GO and chlorinated phenolic compounds.

Solution pH will have an influence on the surface charge of the adsorbent and the dissociation level of the organic compounds. The original pH of 2,4,6-TCP solution was around 5, adding GO to the solution had no much change in the pH of the solution. In the present work, tested compounds have different pK_a values, among these 2,4,6-TCP has the lowest pK_a (6.18), and TBBPA has two proton bonding sites, carboxyl, and piperazinyl group with pK_a values of 7.5 and 8.5, leading to the consideration of pH effect (Zhang et al., 2013). In Fig. 7a, the adsorption capacity values of 2,4,6-TCP on GO nanoflakes showed a slight decrease with increasing pH lower than its pK_a , which could result from some partly deprotonated TCP. However, when pH increased to 9, the adsorption capacity seemed to increase back to that at pH 4, indicating the electrostatic interactions occurred since most TCP were deprotonated. A similar pattern was also observed for TBBPA.

On the other hand, the properties of GO could explain the adsorption mechanism due to the hydrogen bonding or π - π interaction. Investigating the solution pH over pH_{zpc} (Liu et al., 2014), the adsorption enhancement on GO could result from its hydrophobic interaction with GO and HDA interaction by the hydrogen-bond donor of protonated TCP. In the case of TBBPA, its uptake decreased with the increase of TBBPA equilibrium concentrations at pH > 7. The adsorption of TBBPA declined due to the anionic form being less hydrophobic to attach GO surface than the neutral one (Gao et al., 2012) (Fig. 8).

From the view of molecular interaction by FTIR spectroscopy, the change of peaks and their intensities were observed in the whole range of the interaction between PCs and GO after the adsorption (Fig. 9a and b). The interaction between PCs and the oxygen-carrying functional group was confirmed by the presence of peaks at 3479 cm^{-1} , 1632 and 1070 cm^{-1} respectively, these peaks confirm the adsorption of PCs were held on GO due to the hydrogen bonding. The FTIR spectra of BPA, phenol, TBBPA, and 4-NP on GO exhibit bands at 1439 cm^{-1} due to the stretching vibrations of aromatic rings, while the peak at 3479 cm^{-1} is due to —OH stretching (Li et al., 2008). A small shift in the region between 1500 and 1700 cm^{-1} was observed after adsorption, Zhao et al. (2011) observed that the —OH bond of single-walled carbon nanotubes after adsorption from 3320 cm^{-1} to 3479 cm^{-1} for phenol and aniline. Phatthanakittiphong and Seo (2016) observed the shift in peak intensity from 1620 cm^{-1} to 1632 cm^{-1} , confirming the π - π interaction to be the main governing mechanism for adsorption of BPA on GO. The peaks of alkoxy C—O shifted from 1051 to 1042 cm^{-1} and also the peak shift from 3407 to

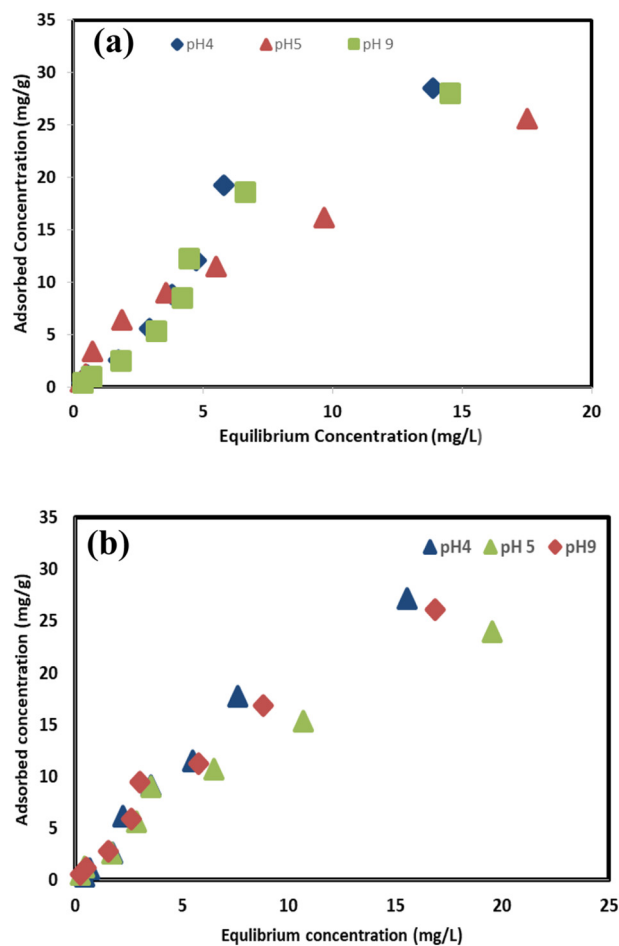


Fig. 8. (a) The effect of pH on adsorption isotherms of 2,4,6-TCP (b) the effect of pH on adsorption isotherms of TBBPA on GO.

1378 cm^{-1} due to O—H bonding after adsorption (Jiang et al., 2015; Wu et al., 2014), similar to our study.

To understand the adsorption process, extensive study has been performed to analyze the adsorption capacity of different carbon-based nanomaterial adsorbents. The adsorption capacity for the removal of compounds used in our study in comparison with the other data in literature has been reported in Table S3. Although Zhang et al. (2013) found a high adsorption capacity of TBBPA, 115.7 mg/g, it could result from the less surface area of our synthesized GO. Phatthanakittiphong and Seo (2016) synthesized GO using Improved Hummers method and found the maximum adsorption capacity towards BPA was around 50 mg/g less than other carbon-based nanomaterials, which is similar to our study. In comparison our measured q_m value of 2,4,6-TCP adsorption on GO was twice to that done by Wang et al. (2014c), which could result from the less hydrophobic surface properties of our GO (Petrie et al., 2015). Graphene has less hydrophilic moieties on its surface and the reduction process of GO (RGO) decreased substantially the oxygen-containing functional groups on the surfaces of GO, leading to the increase of the π - π interaction between graphene/RGO and the adsorbate (Chen et al., 2007; Pei et al., 2013; Sheng et al., 2010; Wang et al., 2014d).

3.5. Environmental risk of GO

The fate of nanoscale materials is preliminary governed by its stability in natural and engineered aquatic system (Hsiung et al., 2016; Peng et al., 2017). Our GO nanoflakes prepared by improved Hummers method has a good water disperse ability, which could be due to the presence of hydrophilic functional groups on its surface. GO also serves

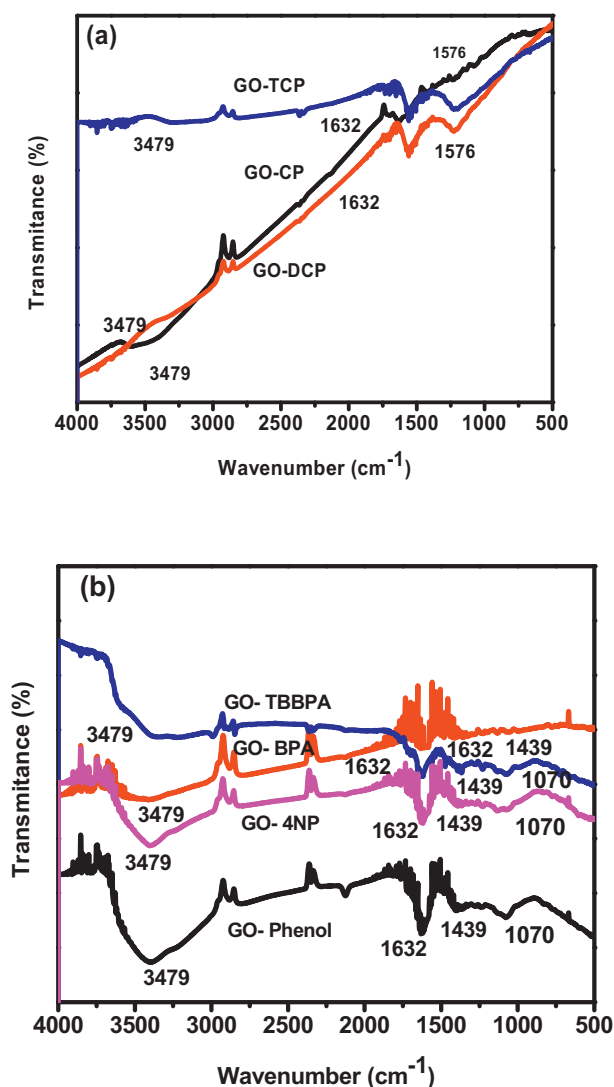


Fig. 9. FTIR spectra after adsorption of (a) 4-chlorophenol, 2,4-dichlorophenol and 2,4,6-trichlorophenol and (b) bisphenol A, phenol, TBBPA and 4-nonylphenol on GO.

as an excellent dispersion agent for various nanomaterials (Li et al., 2008). Carbonaceous materials such as black carbons (BCs) raise a public concern due to their wide application and also its important role in biogeochemical processes due to its high mobility in the environment it affects the transport of the adsorbed contaminants in addition to its stability (Lian and Xing, 2017). Like BCs, there are growing concerns that carbon-based nanomaterials such as GOs will enter natural water bodies due to its wide range of applications. GO also interact with the natural substances present in the water changing the composition of the substance and its fate, molecular dynamics simulation tool was used to investigate the aggregation of GO and observed that hydrogen bond formed between water and GO at higher pH increased its hydrophilicity (Tang et al., 2017). GO also tend to be stable in natural water systems and accumulates in the silica surface of groundwater system (Chowdhury et al., 2013).

As GO nanoflakes are composed of benzene rings with oxygen-carrying functional groups on its plan, considering the effect of various functional groups as necessary. Wang et al. (2016) studied the stability of GOs in water to understand their fate in the environment and evaluate their environmental risks, by adding some electrolytes NaCl and MgCl_2 , leading to the formation of irreversible coagulants when added in excess; however, the GO dispersion can still remain stable when adding excess AlCl_3 . Even in the presence of 0.01 M CaCl_2 , our GO

nanoflakes with different concentrations of BPA were suspended well (Fig. 4). In the literature, since the concentration of GO in the environment could be around several ng/L to $\mu\text{g/L}$ now and the amount of contaminant adsorbed to GO is even two orders of magnitude smaller in this study, the adsorption to natural organic and inorganic material could play a more important role. However, the accidental release of GO into the environment could occur due to the rapid development and large applications of nanotechnology. Furthermore, for the stable GO we prepared, once GOs adsorbed organic compounds can suspend well in water and then transport in the aquatic environment, implicating the expansion of organic contaminants in the environment through the adsorption on well-suspended carbonaceous nanomaterials such as GOs.

4. Conclusions

The present study was conducted to investigate the use of synthesized GO nanoflakes for adsorption of phenolic and emerging contaminants from water. GO nanoflakes, we synthesized can suspend very well in water for months even with these organic contaminants. The adsorption kinetics was fitted with the pseudo second-order model slightly better than the pseudo first-order one. The adsorption isotherms were described by Langmuir isotherm slightly better than Freundlich one. The maximum adsorption capacity of these seven PCs on GO nanoflakes was around 19–30 mg/g in our studied concentration range, which was around twice of that measurements in the literature. Adsorption mechanism of PCs on GO was mainly dominated by Van der Waals force and π - π interaction. The interaction of hydrogen-bond donor and acceptor (HDA) also contributed the adsorption since GO had oxygen carrying functional groups. Phenol has the highest hydrophobicity, strong π - π interaction, and HDA ability from its hydroxyl functional group. Since the high stability of GO nanoflakes in water could increase the hazardous potential once organic contaminants such as ECs adsorbed on them, these better understandings of their adsorption behaviors can facilitate the fate prediction of organic contaminants in the aquatic environment. Although adsorption is a complex function of adsorbent properties and adsorbate molecular structure, a predictable adsorption of these conventional and emerging organic contaminants on this well-characterized GO was observed.

Acknowledgments

The authors thank Ministry of Science and Technology, Taiwan for financial support under Contract No. NSC 102-2221-E-002-015-MY3 and 106-2221-E-002-043-MY3, and Ministry of Human Resource and Development, India for the fund to support Dr. Hepsiba Catherine.

Appendix A. Supplementary data

Supplementary data to this article can be found online at <https://doi.org/10.1016/j.scitotenv.2018.03.389>.

References

Ahmed, F., Rodrigues, D.F., 2013. Investigation of acute effects of graphene oxide on wastewater microbial community: a case study. *J. Hazard. Mater.* 256–257, 33–39.

Apul, O.G., Wang, Q., Zhou, Y., Karanfil, T., 2013. Adsorption of aromatic organic contaminants by graphene nanosheets: comparison with carbon nanotubes and activated carbon. *Water Res.* 47, 1648–1654.

Bele, S., Samanidou, V., Deliyanni, E., 2016. Effect of the reduction degree of graphene oxide on the adsorption of bisphenol A. *Chem. Eng. Res. Des.* 109, 573–585.

Chen, W., Duan, L., Zhu, D., 2007. Adsorption of polar and nonpolar organic chemicals to carbon nanotubes. *Environ. Sci. Technol.* 41, 8295–8300.

Chowdhury, S., Balasubramanian, R., 2014. Recent advances in the use of graphene-family nanoadsorbents for removal of toxic pollutants from wastewater. *Adv. Colloid Interf. Sci.* 204, 35–56.

Chowdhury, I., Duch, M.C., Mansukhani, N.D., Hersam, M.C., Bouchard, D., 2013. Colloidal properties and stability of graphene oxide nanomaterials in the aquatic environment. *Environ. Sci. Technol.* 47, 6288–6296.

Dimiev, Ayrat M., Tour, James M., 2014. Mechanism of Graphene Oxide Formation. 8 pp. 3060–3068.

Doudrick, K., Nosaka, T., Herckes, P., Westerhoff, P., 2015. Quantification of graphene and graphene oxide in complex organic matrices. *Environ. Sci.: Nano* 2, 60–67.

Dreyer, D.R., Park, S., Bielawski, C.W., Ruoff, R.S., 2010. The chemistry of graphene oxide. *Chem. Soc. Rev.* 39, 228–240.

Gao, Y., Li, Y., Zhang, L., Huang, H., Hu, J., Shah, S.M., et al., 2012. Adsorption and removal of tetracycline antibiotics from aqueous solution by graphene oxide. *J. Colloid Interface Sci.* 368, 540–546.

Hsiung, C.-E., Lien, H.-L., Galliano, A.E., Yeh, C.-S., Shih, Y.-H., 2016. Effects of water chemistry on the destabilization and sedimentation of commercial TiO₂ nanoparticles: role of double-layer compression and charge neutralization. *Chemosphere* 151, 145–151.

Jiang, T., Liu, W., Mao, Y., Zhang, L., Cheng, J., Gong, M., et al., 2015. Adsorption behavior of copper ions from aqueous solution onto graphene oxide–CdS composite. *Chem. Eng. J.* 259, 603–610.

Johra, F.T., Lee, J.-W., Jung, W.-G., 2014. Facile and safe graphene preparation on solution based platform. *J. Ind. Eng. Chem.* 20, 2883–2887.

Kalita, G., Qi, L., Namba, Y., Wakita, K., Umeno, M., 2011. Femtosecond laser induced micropatterning of graphene film. *Mater. Lett.* 65, 1569–1572.

Konkena, B., Vasudevan, S., 2012. Understanding aqueous dispersibility of graphene oxide and reduced graphene oxide through pK_a measurements. *J. Phys. Chem. Lett.* 3, 867–872.

Krishnamoorthy, K., Veerapandian, M., Yun, K., Kim, S.J., 2013. The chemical and structural analysis of graphene oxide with different degrees of oxidation. *Carbon* 53, 38–49.

Li, D., Muller, M.B., Gilje, S., Kaner, R.B., Wallace, G.G., 2008. Processable aqueous dispersions of graphene nanosheets. *Nat. Nanotechnol.* 3, 101–105.

Lian, F., Xing, B., 2017. Black carbon (biochar) in water/soil environments: molecular structure, sorption, stability, and potential risk. *Environ. Sci. Technol.* 51, 13517–13532.

Liang, S., Shen, Z., Yi, M., Liu, L., Zhang, X., Ma, S., 2016. In-situ exfoliated graphene for high-performance water-based lubricants. *Carbon* 96, 1181–1190.

Liu, F.F., Zhao, J., Wang, S., Du, P., Xing, B., 2014. Effects of solution chemistry on adsorption of selected pharmaceuticals and personal care products (PPCPs) by graphenes and carbon nanotubes. *Environ. Sci. Technol.* 48, 13197–13206.

Liu, F.F., Zhao, J., Wang, S., Xing, B., 2016. Adsorption of sulfonamides on reduced graphene oxides as affected by pH and dissolved organic matter. *Environ. Pollut.* 210, 85–93.

Mejias Carpio, I.E., Santos, C.M., Wei, X., Rodrigues, D.F., 2012. Toxicity of a polymer-graphene oxide composite against bacterial planktonic cells, biofilms, and mammalian cells. *Nanoscale* 4, 4746–4756.

Moreno-Castilla, C., 2004. Adsorption of organic molecules from aqueous solutions on carbon materials. *Carbon* 42, 83–94.

Pei, Z., Li, L., Sun, L., Zhang, S., Shan, X.-q., Yang, S., et al., 2013. Adsorption characteristics of 1,2,4-trichlorobenzene, 2,4,6-trichlorophenol, 2-naphthol and naphthalene on graphene and graphene oxide. *Carbon* 51, 156–163.

Peng, B., Chen, L., Que, C., Yang, K., Deng, F., Deng, X., et al., 2016. Adsorption of antibiotics on graphene and biochar in aqueous solutions induced by pi-pi interactions. *Sci. Rep.* 6, 31920.

Peng, Y.H., Tsai, Y.C., Hsiung, C.E., Lin, Y.H., Shih, Y.H., 2017. Influence of water chemistry on the environmental behaviors of commercial ZnO nanoparticles in various water and wastewater samples. *J. Hazard. Mater.* 322, 348–356.

Perumbilavil, S., Sankar, P., Priya Rose, T., Philip, R., 2015. White light Z-scan measurements of ultrafast optical nonlinearity in reduced graphene oxide nanosheets in the 400–700 nm region. *Appl. Phys. Lett.* 107, 051104.

Petrie, B., McAdam, E.J., Whelan, M.J., Lester, J.N., Cartmell, E., 2013. The determination of nonylphenol and its precursors in a trickling filter wastewater treatment process. *Anal. Bioanal. Chem.* 405, 3243–3253.

Petrie, B., Barden, R., Kasprzyk-Hordern, B., 2015. A review on emerging contaminants in wastewaters and the environment: current knowledge, understudied areas and recommendations for future monitoring. *Water Res.* 72, 3–27.

Phatthanakitiphong, T., Seo, G.T., 2016. Characteristic evaluation of graphene oxide for bisphenol A adsorption in aqueous solution. *Nanomaterials (Basel)* 6.

Rivera-Utrilla, J., Sanchez-Polo, M., Ferro-Garcia, M.A., Prados-Joya, G., Ocampo-Perez, R., 2013. Pharmaceuticals as emerging contaminants and their removal from water. *A review. Chemosphere* 93, 1268–1287.

Sahu, R.S., Bindumadhavan, K., R-a, Doong, 2017. Boron-doped reduced graphene oxide-based bimetallic Ni/Fe nanohybrids for the rapid dechlorination of trichloroethylene. *Environ. Sci.: Nano* 4, 565–576.

Shen, Y., Fang, Q., Chen, B., 2015. Environmental applications of three-dimensional graphene-based macrostructures: adsorption, transformation, and detection. *Environ. Sci. Technol.* 49, 67–84.

Sheng, G.D., Shao, D.D., Ren, X.M., Wang, X.Q., Li, J.X., Chen, Y.X., et al., 2010. Kinetics and thermodynamics of adsorption of ionizable aromatic compounds from aqueous solutions by as-prepared and oxidized multiwalled carbon nanotubes. *J. Hazard. Mater.* 178, 505–516.

Sophia, A.C., Lima, E.C., 2018. Removal of emerging contaminants from the environment by adsorption. *Ecotoxicol. Environ. Saf.* 150, 1–17.

Sun, Y., Yang, S., Zhao, G., Wang, Q., Wang, X., 2013. Adsorption of polycyclic aromatic hydrocarbons on graphene oxides and reduced graphene oxides. *Chem. Asian J.* 8, 2755–2761.

Tang, H., Zhao, Y., Yang, X., Liu, D., Shao, P., Zhu, Z., et al., 2017. New insight into the aggregation of graphene oxide using molecular dynamics simulations and extended Derjaguin-Landau-Verwey-Overbeek theory. *Environ. Sci. Technol.* 51, 9674–9682.

Thirumal, V., Pandurangan, A., Jayavel, R., Ilangoan, R., 2016. Synthesis and characterization of boron doped graphene nanosheets for supercapacitor applications. *Synth. Met.* 220, 524–532.

- Tso, C.P., Zhong, C.M., Shih, Y.H., Tseng, Y.M., Wu, S.C., Doong, R.A., 2010. Stability of metal oxide nanoparticles in aqueous solutions. *Water Sci. Technol.* 61, 127–133.
- Veerakumar, P., Tharini, J., Ramakrishnan, M., Panneer Muthuselvam, I., Lin, K.-C., 2017. Graphene oxide nanosheets as an efficient and reusable sorbents for eosin yellow dye removal from aqueous solutions. *ChemistrySelect* 2, 3598–3607.
- Wang, F., Haftka, J.J., Sinnige, T.L., Hermens, J.L., Chen, W., 2014a. Adsorption of polar, non-polar, and substituted aromatics to colloidal graphene oxide nanoparticles. *Environ. Pollut.* 186, 226–233.
- Wang, J., Chen, Z., Chen, B., 2014b. Adsorption of polycyclic aromatic hydrocarbons by graphene and graphene oxide nanosheets. *Environ. Sci. Technol.* 48, 4817–4825.
- Wang, J., Gao, X., Wang, Y., Gao, C., 2014c. Novel graphene oxide sponge synthesized by freeze-drying process for the removal of 2,4,6-trichlorophenol. *RSC Adv.* 4, 57476–57482.
- Wang, X., Huang, S., Zhu, L., Tian, X., Li, S., Tang, H., 2014d. Correlation between the adsorption ability and reduction degree of graphene oxide and tuning of adsorption of phenolic compounds. *Carbon* 69, 101–112.
- Wang, M., Niu, Y., Zhou, J., Wen, H., Zhang, Z., Luo, D., et al., 2016. The dispersion and aggregation of graphene oxide in aqueous media. *Nanoscale* 8, 14587–14592.
- Wu, Z., Zhong, H., Yuan, X., Wang, H., Wang, L., Chen, X., et al., 2014. Adsorptive removal of methylene blue by rhamnolipid-functionalized graphene oxide from wastewater. *Water Res.* 67, 330–344.
- Wu, Z., Yuan, X., Zhong, H., Wang, H., Zeng, G., Chen, X., et al., 2016. Enhanced adsorptive removal of p-nitrophenol from water by aluminum metal-organic framework/reduced graphene oxide composite. *Sci. Rep.* 6, 25638.
- Xu, J., Wang, L., Zhu, Y., 2012. Decontamination of bisphenol a from aqueous solution by graphene adsorption. *Langmuir* 28, 8418–8425.
- Yao, Z.T., Yuan, W.Y., Xie, Z.M., Tang, J.H., 2015. A novel debromination of tetrabromobisphenol A (TBBPA) by hydrothermal treatment with reactive minerals. *Appl. Mech. Mater.* 768, 612–621.
- Yu, L., Zhang, Y., Zhang, B., Liu, J., 2014. Enhanced antibacterial activity of silver nanoparticles/halloysite nanotubes/graphene nanocomposites with sandwich-like structure. *Sci. Rep.* 4, 4551.
- Zhang, Y., Tang, Y., Li, S., Yu, S., 2013. Sorption and removal of tetrabromobisphenol A from solution by graphene oxide. *Chem. Eng. J.* 222, 94–100.
- Zhao, G., Li, J., Ren, X., Chen, C., Wang, X., 2011. Few-layered graphene oxide nanosheets as superior sorbents for heavy metal ion pollution management. *Environ. Sci. Technol.* 45, 10454–10462.
- Zhu, S., Liu, Y.G., Liu, S.B., Zeng, G.M., Jiang, L.H., Tan, X.F., et al., 2017. Adsorption of emerging contaminant metformin using graphene oxide. *Chemosphere* 179, 20–28.